Stomach-specific Calpain, nCL-2/calpain 8, Is Active Without Calpain Regulatory Subunit, and Oligomerizes Through C2-like Domains*

Shoji Hata[1], Naoko Doi[1,2], Fujiko Kitamura[1], Hiroyuki Sorimachi[1,2]

[1]Department of Enzymatic Regulation for Cell Functions (Calpain Project), The Tokyo Metropolitan Institute of Medical Science (Rinshoken), Tokyo 113-8613, [2]CREST, Japan Science and Technology Agency (JST), Saitama 332-0012, Japan

Running title: Stomach-specific calpain oligomerizes via C2-like Domains

Address correspondence to: Hiroyuki Sorimachi, Department of Enzymatic Regulation for Cell Functions, The Tokyo Metropolitan Institute of Medical Science (Rinshoken), 3-18-22 Honkomagome, Bunkyo-ku, Tokyo 113-8613, Japan; FAX: +81-3-3823-2359; E-mail: sorimach@rinshoken.or.jp.

Calpains constitute a family of intracellular Ca^{2+}-regulated cysteine proteases that are indispensable in the regulation of a wide variety of cellular functions. The improper activation of calpain causes lethality or various disorders, such as muscular dystrophies and tumor formation. nCL-2/calpain 8 is predominantly expressed in the stomach, where it appears to be involved in membrane trafficking in the gastric surface mucus cells (pit cells). Although the primary structure of nCL-2 is quite similar to that of the ubiquitous m-calpain large subunit, the enzymatic properties of nCL-2 have never been reported. Here, to characterize nCL-2, the recombinant protein was prepared using an *E. coli* expression system and purified to homogeneity. nCL-2 was stably produced as a soluble and active enzyme without the conventional calpain regulatory subunit (30K). Purified nCL-2 showed Ca^{2+}-dependent activity, with half-maximal activity at about 0.3 mM Ca^{2+}, similar to that of m-calpain, whereas its optimal pH and temperature were comparatively low. Immunoprecipitation analysis revealed that nCL-2 exists in both monomeric and homo-oligomeric forms, but not as a heterodimer with 30K or 30K-2, and that the oligomerization occurs through domains other than the 5EF-hand domain IV, most probably through domain III, suggesting a novel regulatory system for nCL-2.

Calpain (Clan CA-C2, EC 3.4.22.17) is an intracellular Ca^{2+}-regulated cysteine protease, comprising a superfamily with members in almost all eukaryotes and some bacteria (1-3). Calpains regulate a wide variety of cellular functions including the cell cycle, signal transduction, apoptosis, and membrane trafficking, through the limited proteolysis of their substrates (1,2,4,5). Dysregulation of calpain activity and/or defective mutations in calpain genes cause lethality (6-8) or a variety of pathological phenotypes, which include muscular dystrophies in mammals (9,10), degeneration in the developing optic lobes of drosophila (11), inadaptability to alkaline conditions in fungi and yeasts (12,13), masculinization of nematode hermaphrodites (14), and defective aleurone cell development in maize

(15). These observations clearly indicate calpain is indispensable physiologically; however, the specific physiological functions of calpains and the molecular mechanisms underlying their functions remain unclear.

The mammalian calpain family comprises products from 14 independent genes, and can be classified into typical and atypical members according to their domain structures (2,3). The ubiquitous μ- and m-calpains, well-characterized typical calpains in mammals, are hetero-dimers composed of a distinct 80-kDa large catalytic subunit (abbreviated here to μCL and mCL, respectively; also known as calpain 1 and 2) and a common 30-kDa small regulatory subunit (30K). The large and small subunits contain four (I–IV) and two (V and VI) domains, respectively: the regulatory N-terminal domain (I), the protease domain (II), the C2-domain-like Ca^{2+}/phospholipid-binding domain (III), the penta-EF-hand (PEF) domains (IV and VI), which are missing in atypical calpains, and the Gly-clustering hydrophobic domain (V). The C-terminal fifth EF-hand motifs in domains IV and VI cannot bind Ca^{2+}, and interact with each other to form the hetero-dimer. Domain IV is also reported to function in the recognition of substrates and regulatory molecules (16-18).

In the absence of Ca^{2+}, the protease domain (II) is separated into two subdomains, IIa and IIb, and residues in the catalytic triad are prevented from assuming the correct positions for hydrolysis. The binding of Ca^{2+} to domains IIa, IIb, III, IV, and VI induces conformational changes that allow domain II to form a single active domain (19-23). Previous analyses revealed that μCL and mCL show full activity in the absence of 30K if correctly folded (24), and cells from 30K gene-deficient mice, which die at E10.5-11.5, show neither detectable μ- or m-calpain activity nor detectable μCL or mCL protein, even though their mRNAs are expressed normally (7,8). These results indicated that 30K functions as a molecular chaperon *in vivo*, at least for μCL and mCL.

nCL-2/calpain 8, identified as a stomach-specific calpain, is a typical calpain with four domains (25) (see Fig. 3B). nCL-2 is most similar to mCL (amino acid identities in the full-length protein and in domains II and IV are 61.5%, 73.4%, and 51.8%, respectively). Possible functions for nCL-2 in the pituitary gland and in the embryogenesis of *Xenopus laevis* have been reported (26,27). We recently showed that, in the stomach, nCL-2 as well as nCL-4/calpain 9, a digestive tract-specific calpain, are expressed specifically in the mucus-secreting pit cells, quite unlike the μ- and m-calpains, which are expressed diffusely in all cells, and that nCL-2 may be involved in the regulation of vesicle trafficking in the gastric surface mucus cells (pit cells) (28). These reports highlight potentially important nCL-2 functions that cannot be compensated for by μ- and m-calpains, not only in the stomach but also in other tissues.

However, the enzymatic properties of nCL-2, including its regulatory mechanisms, have not been reported, except for one yeast two-hybrid analysis suggesting that nCL-2 does not interact with 30K despite the high similarity between nCL-2 and mCL (29). Thus, in this study, using *E. coli*–expressed and purified nCL-2, the detailed biochemical properties of this enzyme were

examined, and several unique characteristics were revealed. Unexpectedly, nCL-2 was found to exist as both a monomer and as homo-oligomers, and the domain responsible for oligomerization was, unlike in the μ- and m-calpains, the C2-like domain (III), not the PEF domain (IV), suggesting that nCL-2 has a novel regulatory mechanism.

Experimental Procedures

Materials– Recombinant human μ- and m-calpains, anti-nCL2 polyclonal antibody (previously called anti-nCL2/2'), and mouse gastric mucosal protein were prepared as described previously (28,30). RP2-calpain 8 polyclonal antibody, anti-FLAG (clone M2), anti-HA (clone 6E2), and anti-His monoclonal antibodies were purchased from Triple Point Biologics Inc. (OR, USA), Sigma (MO, USA), Cell Signaling Technology Inc. (MA, USA), and Novagen Inc. (WI, USA), respectively. Protease inhibitors (calpeptin, calpain inhibitor I, calpastatin domain I, E64c, AEBSF, PMSF, TLCK, pepstatin A) were purchased from Sigma, TaKaRa (Kyoto, Japan), and Peptide Institute Inc. (Osaka, Japan). CSTN pep42 (NH_2-EVSDPMSSTYIEELGKREVTIPPKYRELLAKPIGPDDAIDAL-COOH), corresponding to one of reactive sites of human calpastatin, was synthesized by Research Genetics (CA, USA).

Cloning and construction of expression plasmids– cDNAs encoding full-length mouse nCL-2, human and mouse 30K, and human and mouse 30K-2/CAPNS2 were amplified by PCR using *Pfu* turbo DNA polymerase (Stratagene Inc., CA, USA), and the sequences were verified after being subcloned into appropriate vectors. For bacterial expression, the amplified mouse nCL-2 cDNA was ligated into the pCold I vector (TaKaRa) to produce proteins fused with an N-terminal His-tag. For COS7 cell expression, the amplified cDNAs were ligated into a modified pSRD vector (31) to produce proteins fused with an N-terminal FLAG, HA, or myc-tag. The nCL-2 deletion mutants were constructed by introducing termination codons at the appropriate positions using a PCR-mediated site-directed mutagenesis method as previously described (10).

Protein expression in bacterial cells and purification– The constructed pCold I expression plasmids were transformed into *E. coli* BL21/pG-Tf2 (TaKaRa), and the transformants were cultured at 37°C in 3 L of LB medium containing 0.1 mg/ml ampicillin until A_{600} = 0.6. Protein expression was induced by the addition of 0.5 mM isopropyl-thiogalactoside and 5 ng/ml tetracycline (tet) for 24 h at 15°C. Harvested cells were washed once with phosphate-buffered saline, and resuspended in 150 ml of lysis buffer (20 mM Tris-Cl (pH 7.5), 150 mM NaCl, 5 mM imidazole, and 1.4 mM 2-mercaptoethanol (2-ME)), and lysed with a French Press (American Instruments Inc., MA, USA). The cell lysate was spun at 55,000 × g for 20 min, and the recovered supernatant was filtered through a 0.22-μm pore filter (Millipore, MA, USA). The supernatant was then applied by gravity to a 2-ml Ni^{2+}-chelating agarose column (Qiagen, MD, USA) equilibrated with lysis buffer. The column was washed with 10 column volumes of lysis buffer, and then six column volumes of wash buffer (20 mM Tris-Cl (pH 7.5), 150 mM NaCl, 50 mM Imidazole, and

1.4 mM 2-ME). Protein was then eluted with 8 ml of elution buffer (20 mM Tris-Cl, (pH 7.5), 150 mM NaCl, 250 mM Imidazole, and 1.4 mM 2-ME). The eluate was immediately dialyzed against buffer A (20 mM Tris-Cl (pH 7.5), 1 mM EDTA, and 1 mM dithiothreitol (DTT)) at 4^{o}C. The dialyzed sample was further purified by a MonoQ HR10/10 anion-exchange column (GE Healthcare, Tokyo, Japan) with a linear gradient of 0–0.5 M NaCl in buffer A. For gel filtration, the sample was applied to a HiLoad 16/10 Superdex 200 column (GE Healthcare) equilibrated with buffer A containing 150 mM NaCl. The purity of the protein was examined by SDS-PAGE analysis. The peak fraction was stored at 4°C until use.

Proteolysis assay– Proteolytic activity was measured using a fluorogenic substrate, succinyl-Leu-Leu-Val-Tyr-4-methylcoumaryl-7-amide (Suc-LLVY-MCA) (Peptide Institute Inc.). Recombinant nCL-2 (2 μg), μ-calpain (0.1 μg), or m-calpain (0.4 μg) was incubated with 0.1 mM Suc-LLVY-MCA in reaction buffer (0.1 M Tris-Cl (pH7.5), 20 mM 2-ME and 0.2% 3-[(3-cholamidopropyl)dimethyl-ammonio]propanesulfonic acid (CHAPS)), with varying Ca^{2+} concentrations, temperatures, or pH. For pHs other than 7.5, Tris-acetate (pH5.5, 6.0, or 6.8) or Tris-Cl (pH7.0, 7.3, 8.0, 9.0, or 9.5) buffer was used instead of Tris-Cl (pH7.5) buffer. Reactions in 40 μl were stopped by the addition of 40 μl of 10% SDS and 1.2 ml of 0.1 M Tris-Cl (pH 9.0). MCA release by proteolysis was monitored by a spectrofluorophotometer (RF-1500, Shimadzu, Osaka, Japan), with excitation and emission wavelengths at 380 nm and 460 nm, respectively. For the autolysis assay, 1 μg of recombinant nCL-2 was incubated in 10 μl of the reaction buffer with or without 10 mM $CaCl_2$ at 25 or 37°C for the times indicated.

Protein expression in culture cells and Immunoprecipitation– COS7 cells were transfected with 5 μg of the expression plasmids by electroporation, as previously described (31). For immunoprecipitation, the COS7 cells were harvested 48 h after transfection and lysed with lysis buffer (20 mM Tris-Cl (pH 7.5), 150 mM NaCl, 5 mM EDTA, 1% TritonX-100, 0.2 mM PMSF, 10 μg/ml aprotinin, and 10 μM pepstatin A). The lysed cells were spun at 100,000 × g for 20 min and incubated with a 50% slurry of FLAG (M2) agarose (Sigma) for 2 h, then the protein-bound agarose was washed five times with 1 ml of the lysis buffer. The immunoprecipitated proteins were eluted with 0.1 mg/ml FLAG peptide (Sigma) and mixed with SDS sample buffer. For the *in vitro* proteolysis assay, 10 μl of the eluted immunoprecipitated proteins were incubated with 2 μl of 6 × Ca-buffer (20 mM Tris-Cl (pH 7.5), 100 mM $CaCl_2$, and 6 mM DTT) or 2 μl of 6 × EDTA-buffer (20 mM Tris-Cl (pH 7.5), 100 mM EDTA, and 6 mM DTT) at 37°C. The reactions were stopped by the addition of 5 × SDS sample buffer.

Protein sequencing – After SDS–PAGE, the proteins were blotted onto a Pro-Blot membrane (Applied Biosystems, Tokyo, Japan). Target protein bands on the membrane were visualized by Coomassie Brilliant Blue (CBB) G-250 staining, excised, and washed three times with 0.1% (v/v) trifluoroacetic acid in 50% (v/v) methanol and then with absolute methanol. Sequencing was performed using the ABI 491cLC

protein sequencer (Applied Biosystems), according to the manufacturer's instructions.

RESULTS

Preparation of recombinant mouse nCL-2 using an E. coli expression system. To investigate the solubility and expression efficiency of nCL-2, full-length mouse nCL-2 was expressed with or without 30K in *E. coli* BL21(DE3). nCL-2 was abundantly expressed in both cases, and no significant difference was observed in its amount or solubility (data not shown). Therefore, nCL-2 was expressed without 30K for the purpose of purification. To improve the solubility of the nCL-2 in *E. coli*, a tet-on chaperon-inducible BL21/pG-Tf2 strain was used, and active nCL-2 was successfully recovered in a soluble fraction that represented one-third to one-half of the total nCL-2 (Fig.1A, lanes 1 and 2).

Purification of recombinant nCL-2. As described in Experimental Procedures, N-terminally His-tagged recombinant nCL-2 was expressed and purified to homogeneity by Ni^{2+}-chelating agarose and MonoQ anion-exchange column chromatographies in succession (Fig. 1A, lanes 3 and 4). The peak elution of nCL-2 from the MonoQ column was at around 0.2 M NaCl. Approximately 1 mg of recombinant nCL-2 was purified from 3 L of *E. coli* culture, and subjected to further analyses.

Enzymatic properties of recombinant nCL-2. Using the nCL-2 prepared above, the enzymatic characterization of recombinant nCL-2 was performed, in comparison with recombinant human μ- and m-calpains. A fluorogenic substrate, Suc-LLVY-MCA, was used to detect the proteolytic activities. The activity of nCL-2 was Ca^{2+} dependent, and was blocked by known inhibitors of μ- and m-calpains but not by other inhibitors (Figs. 2A & B), demonstrating that nCL-2 possesses characteristics typical of conventional calpains. The concentration of Ca^{2+} required for half-maximal activity was about 0.3 mM, almost identical to that of m-calpain (Fig. 2A). The calculated specific activity was a 40th and a 25th of that of μ- and m-calpain, respectively. The specific activity of the caseinolysis of nCL-2 was also lower than those of μ- and m-calpain (data not shown).

To exclude a possibility that the proteolytic activity observed is due to host protease(s) contaminating in the final nCL-2 fraction, the Suc-LLVY-MCA assay was performed for the lysates of BL21/pG-Tf2 cells transformed with mock (pCold empty vector), or expression vectors for inactive nCL-2 (nCL-2:C105S, in which the active site Cys-105 was mutated to Ser), or WT nCL-2. As a result, the mock- and nCL-2:C105S-transformed cell lysates showed virtually no activity (0.25 ± 0.01 and 1.97 ± 0.02 fluorescence units (FU), respectively) in the presence of Ca^{2+}, whereas WT nCL-2-transformed cell lysate showed >200 times their activities (403.07 ± 0.81 FU) (Fig. 1B). Furthermore, "mock purification" was also performed using the mock-transformed cell lysate (Fig. 1C, S2) in the same manner as that for WT nCL-2 (Fig. 1C, S1). As a result, the final Mono Q fractions (Fig. 1C, lanes E1–E3) around 0.2 M NaCl, where WT nCL-2 was mainly eluted, showed no activity. Thus, the possibility of host protease activities

was excluded.

The optimal temperature for nCL-2 activity was 20°C (Fig. 2C), which was similar to that for μ- and m-calpain under our assay conditions, and to that reported previously for nCL-4 (32,33). The time courses of nCL-2 activity at various temperatures showed that the initial rates were maximal at 30 to 37°C, while maximal activity was achieved at 15°C (Fig. 2D). The low optimal temperature for nCL-2 indicates that it is unstable at higher temperatures in the presence of Ca^{2+}. The optimal pH for nCL-2 activity was 6.0, which is lower than the optimal pHs for conventional calpains (Fig. 2E).

Autolytic properties of nCL-2. The autolysis of nCL-2 was examined by SDS-PAGE analysis, as shown in Fig. 3A. Various breakdown products appeared in a time-dependent manner, and were confirmed to be autolytic fragments of nCL-2 by western blot analysis (Fig. 3B). By N-terminal sequencing of a 43-kDa fragment (Fig. 3A, arrowhead e), one of the autolysis sites was determined to be between Ala-5 and Ala-6. Given its molecular weight, the C-terminus of this fragment was in or near the acidic loop in domain III (Fig. 3C, e).

The autolytic fragment just below the 81-kDa full-length band (Figs. 3A & 3B, arrowhead a) reacted with the anti-nCL2 but not the anti-His antibody. Based on this and its molecular weight (ca. 79 kDa), this autolytic fragment probably spanned from Ala-6 to the C-terminus (Fig. 3C, a).

Autolytic fragments of 63 kDa (Figs. 3A & 3B, arrowhead b) and 41 kDa (arrowhead f) reacted with the anti-nCL2 and RP2-calpain 8 (anti-domain III) antibodies, and with only the anti-nCL2 antibody, respectively. This indicates that the 63-kDa and 41-kDa fragments extend from Ala-6 to the second EF-hand motif (EF-2) in domain IV and to the beginning of domain III, respectively (Fig. 3C, b and f). Autolytic fragments of 45 kDa and 44 kDa (Figs. 3A & 3B, arrowheads c and d) reacted with the anti-nCL2 and anti-His, but not the RP-calpain 8 antibodies, indicating that these fragments extend from the N-terminus to the acidic loop in domain III and to the beginning of domain III, respectively (Fig. 3C, c and d).

In summary, the autolytic sites of nCL-2 include the N-terminus, the N-terminal parts of domain III, and EF-2 in domain IV.

nCL-2 exists as a monomer and homo-oligomer. The finding that 30K was not required for nCL-2 activity prompted us to investigate the tertiary structure of nCL-2. To examine whether nCL-2 exists as a monomer or homo-oligomer, the purified nCL-2 was subjected to gel filtration column chromatography. As shown in Fig. 4A, nCL-2 was eluted with peaks at positions corresponding to about 80 kDa and 160 kDa. This result indicates that nCL-2 is present as both a monomer and homo-oligomers, and that the monomer and homodimer forms predominate. Suc-LLVY-MCA hydrolyzing activities of both fractions were measured, and the calculated specific activity of the peak fraction at about 160 kDa was about 1/15 of that at about 80 kDa.

To confirm the homo-oligomerization of nCL-2, immunoprecipitation analysis was performed. Full-length mouse nCL-2 fused with an N-terminal FLAG, HA, or myc-tag were co-expressed in COS7 cells; the cell lysate was

spun in an ultracentrifuge and then immunoprecipitated using the appropriate antibodies. The m-calpain subunits, FLAG-30K and HA-mCL, were used as controls. As shown in Fig. 4C, HA-mCL was co-precipitated with FLAG-30K (lane 2), whereas HA-nCL-2 was not (lane 5), consistent with the yeast two-hybrid results described above. These results indicated that this method was applicable for detecting the protein interactions of interest.

When FLAG-nCL-2 and HA-nCL-2 were co-expressed in COS7 cells, HA-nCL-2 was co-precipitated with FLAG-nCL-2 (Fig. 4D, lanes 1–3). To confirm this interaction, the combination of FLAG-nCL-2 and myc-nCL-2 was also tested, and yielded consistent results (Fig. 4D, lanes 4 and 5). Furthermore, to exclude a possibility that observed co-precipitation is an artifact due to overexpression, FLAG-nCL-2 and HA-nCL-2 were co-expressed in COS7 cells at very low levels, even lower than the physiological levels (Fig. 4E, anti-nCL2, lanes 1 vs 2 and 3). Even under this condition, co-precipitation was observed (Fig. 4E, IP: FLAG, anti-HA, lane 3).

nCL-2 oligomerization is not through Domain IV but through Domain III. To investigate which domain is required for the homo-oligomer formation of nCL-2, several truncation mutants of nCL-2 (Fig. 4B) were used in the immunoprecipitation experiment. Since the C-terminal fifth EF-hand motif (EF-5) in domains IV and VI is critical for the heterodimer formation of μ- and m-calpains, we first tested whether the EF-5 of nCL-2 was necessary for oligomerization. When a tagged EF-5 deletion mutant (Fig. 4B, FLAG- or HA-ΔEF5) was co-expressed with full-length nCL-2 or its ΔEF5 mutant, the ΔEF5 mutant was co-precipitated with the ΔEF5 mutant as well as with full-length nCL-2 (Fig. 4F, lanes 6–8; Table 1), indicating that EF-5 is not required for the homo-oligomerization of nCL-2.

Therefore, to identify the novel domain(s) critical for the homo-oligomer formation, domain IV- and domain III/IV-truncated mutants (Fig. 4B, ΔdIV and ΔdIII+IV, respectively) were tested. The ΔdIV mutant was co-precipitated with the ΔdIV mutant (Fig. 5A, lane 3) as well as with full-length nCL-2 (Fig. 5B, lanes 3 and 8; Table 1). On the other hand, the ΔdIII+IV mutant showed almost no interaction with the ΔdIII+IV mutant or with full-length nCL-2 (Fig. 5A, lane 6; 5B, lanes 5 and 10; Table 1). Consistent with these results, HA-domain IV of nCL-2 (Fig. 4B, dIV) was co-precipitated with neither FLAG-full-length nCL-2 nor FLAG-dIV of nCL-2 (Fig. 5C, lanes 3 and 5; Table 1). These results indicate that domain IV is dispensable and domain III is necessary for the oligomer formation of nCL-2.

To confirm the involvement of domain III in nCL-2 oligomerization, FLAG-domain III of nCL-2 (Fig. 4B, dIII) was co-expressed with HA-full-length nCL-2 or HA-dIII of nCL-2. The dIII expression was very faint (Fig. 5C, lysate, lanes 6 and 7), probably because domain III alone is unstable in nature, as previously reported for rat mCL domain III (34). As shown in Fig. 5C, lanes 8 and 10, FLAG-full-length nCL-2 and FLAG-dIII co-precipitated HA-dIII, although the signal was not as clear as in the co-precipitation experiments using full-length nCL-2 or the ΔdIV mutants (Figs. 5A & B; Table 1). These results strongly suggest that nCL-2 oligomerizes through domain III, and

that domain I and/or II may also be required for the proper conformation for binding (Table 1).

Effect of oligomerization on nCL-2 activity. To examine the effect of homo-oligomer formation on nCL-2 autolysis, HA-nCL-2 was co-expressed with FLAG-nCL-2, immunoprecipitated using an anti-FLAG antibody, and incubated in the absence or presence of Ca^{2+}, followed by western blot analysis using anti-FLAG or anti-HA antibodies. As shown in Fig. 6A, both FLAG-nCL-2 and HA-nCL-2 showed Ca^{2+}-dependent autolysis in the same manner.

Next, to investigate whether or not Ca^{2+} induces dissociation of the nCL-2 homo-oligomer, the HA- and FLAG-nCL-2 oligomers were bound to anti-FLAG agarose, incubated with or without Ca^{2+}, washed, and eluted with FLAG-peptide to see if HA-nCL-2 was associated with or dissociated from the bound FLAG-nCL-2 protein. In this experiment, to avoid the autolysis of nCL-2 during incubation with Ca^{2+}, inactive nCL-2:C105S (nCL-2CS) was used. As shown in Fig. 6B, lanes 3 and 6, HA-nCL-2CS was detected at the same level in the absence or presence of Ca^{2+}. These results indicate that the nCL-2 homo-oligomer possesses protease activity without dissociating in the presence of Ca^{2+}.

No interaction of nCL-2 with 30K-2. Recently, 30K-2/CAPNS2, a novel small subunit that shares about 70% amino acid identity with 30K, was identified, and *E. coli*-expressed 30K-2 was shown to form a hetero-dimer with mCL that had enzymatic properties similar to m-calpain (mCL+30K) (35,36). Therefore, it was possible that 30K-2 interacts with and functions as a regulator of nCL-2. When FLAG-30K-2 was expressed in combination with HA-nCL-2 or HA-mCL, HA-mCL but not HA-nCL-2 was co-precipitated with FLAG-30K-2 (Fig. 7, lanes 3 and 6). The interaction of 30K-2 and mCL was weaker than that of 30K and mCL, consistent with previously reported results (35).

DISCUSSION

In this study, we purified *E. coli*-expressed recombinant stomach-specific calpain, nCL-2, and demonstrated that it can be present as a monomer or form a homo-oligomer through domain III. This is the first description of the enzymatic and biochemical properties of nCL-2.

As expected from the high sequence similarity between nCL-2 and mCL, several enzymatic properties of nCL-2 resembled those of m-calpain, such as the Ca^{2+}-dependency and the inhibitor profile of its enzyme activity. However, several other properties were unique to nCL-2, which might reflect its specific expression and functions in the stomach that cannot be compensated for by the μ- and m-calpains. First, nCL-2 showed a low optimal temperature in a long incubation assay, which was similar to that of nCL-4 (33) but different from that of p94Δ (37). Second, the optimal pH for nCL-2 activity was lower than that for the μ- and m-calpains. These properties suggest that nCL-2 evolved to adapt to stomach-specific conditions. Alternatively, these findings may suggest the existence of certain as-yet unidentified stabilizing factor(s) specific for nCL-2 in the stomach.

The specific activity of nCL-2 was much lower than the specific activities of the μ- and

m-calpains. The strong autolytic activity (see Fig. 3A), however, indicated that the low specific activity was not due to partial denaturation of the purified recombinant nCL-2. Moreover, the nCL-2 autolysis was very rapid and extensive; i.e., full-length nCL-2 decayed with a t1/2 of less than 10 sec at 25°C, and it was extensively degraded within 3 min (see Fig. 3A). These properties are distinct from the μ- and m-calpains and from nCL-4+30K (33,38,39), but similar to p94, although p94 apparently does not require Ca^{2+} for autolysis (31). Taken together, these findings suggest that 30K suppresses the autolysis of calpains with which it forms a hetero-dimer, and may indicate that nCL-2 and p94 need to be self-down-regulated very rapidly after their activation, probably to play specific roles in highly differentiated cells like pit cells and muscle cells, respectively.

Alternatively, the low specific activity of nCL-2 for Suc-LLVY-MCA and casein, despite its strong autolytic activity, may indicate that the substrate specificity of nCL-2 is rather different from that of the μ- and m-calpains. In this regard, the identification of *in vivo* substrates for nCL-2, including the candidate molecule β-COP (28), is a very important and emerging future issue.

It was shown that nCL-2 is not co-precipitated with 30K or 30K-2, and that it is stable and has full proteolytic activity without 30K, strongly suggesting that no interaction occurs between nCL-2 and 30K or 30K-2 *in vivo*. As mentioned above, although it cannot be excluded that a regulatory subunit(s) other than 30K and 30K-2 may exist, these results strongly suggest that nCL-2 functions without a regulatory subunit in the stomach. Considering that PEF domain of mCL is more similar to nCL-2 in its primary sequence than to that of nCL-4, but that nCL-4, but not nCL-2, forms a hetero-dimer with 30K, the dimer formation between PEF domains appears to be governed by complicated structural properties that cannot be predicted from the primary sequence.

Importantly, nCL-2 exists not only as a monomer, but also as a homo-oligomer, and the oligomerization is most likely through domain III. The suppressive effect of oligomerization on nCL-2 activity is possible to be related to regulation mechanisms of nCL-2 activity. In other words, as 30K and 30K-2 act as activity suppressors for conventional calpains and nCL-4, oligomerization of nCL-2 may function for the same purpose without 30K or 30K-2. This property has never been reported for any kind of calpain under any experimental condition. However, although the oligomerization was observed even in cells exogenously expressing nCL-2 near the physiological levels, further analysis is required to conclude whether or not native nCL-2 forms oligomers in the stomach.

The homo-oligomer formation through domain III may be supported by the fact that the 3D structure of domain III resembles tumor necrosis factor α (TNFα) (20), which forms a homotrimer (40), although the trimerizing C2-domain has not been reported.

Very recently, it was reported that minicalpains 1, 2, and 9 (domain II) in the presence of Ca^{2+} are structurally different despite their highly conserved sequences, suggesting that typical calpains have rather divergent mechanisms

for their activation and regulation (41). It is possible that there are structural modifications specific to nCL-2 oligomerization involving inter/intra-domain interactions among domains I, II, and III of nCL-2.

Our recent study highlighted a role of nCL-2 in membrane trafficking via its location at the Golgi and interaction with a coatomer subunit of vesicles derived from the Golgi (28). This function implies a possible physiological function of the nCL-2 oligomerization: one nCL-2 molecule could bind directly to scaffold proteins at the membrane, while another nCL-2 in the oligomer, could appropriately proteolyze its substrates at the membrane, such as β-COP. One of the most important issues to be resolved is whether the monomer-oligomer transition is constitutive or inducible *in vivo*, and, if inducible, when it is induced. The answers to such questions will shed light on the physiological functions of nCL-2 and are emerging future issues.

REFERENCES

1. Suzuki, K., Hata, S., Kawabata, Y., and Sorimachi, H. (2004) *Diabetes* **53**, S12-18
2. Goll, D. E., Thompson, V. F., Li, H., Wei, W., and Cong, J. (2003) *Physiol. Rev.* **83**, 731-801
3. Sorimachi, H., and Suzuki, K. (2001) *J. Biochem.* **129**, 653-664
4. Wang, K. K., Larner, S. F., Robinson, G., and Hayes, R. L. (2006) *Curr. Opin. Neurol.* **19**, 514-519
5. Friedrich, P., and Bozoky, Z. (2005) *Biol. Chem.* **386**, 609-612
6. Dutt, P., Croall, D. E., Arthur, S. C., De Veyra, T., Williams, K., Elce, J. S., and Greer, P. A. (2006) *BMC Dev. Biol.* **6**, DOI:10.1186/1471-1213X-1186-1183
7. Arthur, J. S., Elce, J. S., Hegadorn, C., Williams, K., and Greer, P. A. (2000) *Mol. Cell Biol.* **20**, 4474-4481
8. Zimmerman, U. J., Boring, L., Pak, J. H., Mukerjee, N., and Wang, K. K. (2000) *IUBMB Life* **50**, 63-68
9. Richard, I., Broux, O., Allamand, V., Fougerousse, F., Chiannilkulchai, N., Bourg, N., Brenguier, L., Devaud, C., Pasturaud, P., Roudaut, C., Hillaire, D., Passos-Bueno, M.-R., Zats, M., Tischfield, J. A., Fardeau, M., Jackson, C. E., Cohen, D., and Beckmann, J. S. (1995) *Cell* **81**, 27-40
10. Ono, Y., Shimada, H., Sorimachi, H., Richard, I., Saido, T. C., Beckmann, J. S., Ishiura, S., and Suzuki, K. (1998) *J. Biol. Chem.* **273**, 17073-17078
11. Delaney, S. J., Hayward, D. C., Barleben, F., Fischbach, K. F., and Miklos, G. L. (1991) *Proc. Natl. Acad. Sci. U.S.A.* **88**, 7214-7218
12. Denison, S. H., Orejas, M., and Arst, H. N., Jr. (1995) *J. Biol. Chem.* **270**, 28519-28522
13. Futai, E., Maeda, T., Sorimachi, H., Kitamoto, K., Ishiura, S., and Suzuki, K. (1999) *Mol. Gen. Genet.* **260**, 559-568
14. Barnes, T. M., and Hodgkin, J. (1996) *EMBO J.* **15**, 4477-4484

15. Lid, S. E., Gruis, D., Jung, R., Lorentzen, J. A., Ananiev, E., Chamberlin, M., Niu, X., Meeley, R., Nichols, S., and Olsen, O. A. (2002) *Proc. Natl. Acad. Sci. U.S.A.* **99**, 5460-5465
16. Shinozaki, K., Maruyama, K., Kume, H., Tomita, T., Saido, T. C., Iwatsubo, T., and Obata, K. (1998) *Int. J. Mol. Med.* **1**, 797-799
17. Benetti, R., Del Sal, G., Monte, M., Paroni, G., Brancolini, C., and Schneider, C. (2001) *EMBO J.* **20**, 2702-2714
18. Bordone, L., and Campbell, C. (2002) *J. Biol. Chem.* **277**, 26673-26680
19. Hosfield, C. M., Elce, J. S., Davies, P. L., and Jia, Z. (1999) *EMBO J.* **18**, 6880-6889
20. Strobl, S., Fernandez-Catalan, C., Braun, M., Huber, R., Masumoto, H., Nakagawa, K., Irie, A., Sorimachi, H., Bourenkow, G., Bartunik, H., Suzuki, K., and Bode, W. (2000) *Proc. Natl. Acad. Sci. U.S.A.* **97**, 588-592
21. Hata, S., Sorimachi, H., Nakagawa, K., Maeda, T., Abe, K., and Suzuki, K. (2001) *FEBS Lett.* **501**, 111-114
22. Moldoveanu, T., Hosfield, C. M., Lim, D., Elce, J. S., Jia, Z., and Davies, P. L. (2002) *Cell* **108**, 649-660
23. Moldoveanu, T., Hosfield, C. M., Lim, D., Jia, Z., and Davies, P. L. (2003) *Nat. Struct. Biol.* **10**, 371-378
24. Yoshizawa, T., Sorimachi, H., Tomioka, S., Ishiura, S., and Suzuki, K. (1995) *FEBS Lett.* **358**, 101-103
25. Sorimachi, H., Ishiura, S., and Suzuki, K. (1993) *J. Biol. Chem.* **268**, 19476-19482
26. Duan, W. R., Ito, M., Lee, E. J., Chien, P. Y., and Jameson, J. L. (2002) *Biochem. Biophys. Res. Commun.* **295**, 261-266
27. Cao, Y., Zhao, H., and Grunz, H. (2001) *Dev. Growth Differ.* **43**, 563-571
28. Hata, S., Koyama, S., Kawahara, H., Doi, N., Maeda, T., Toyama-Sorimachi, N., Abe, K., Suzuki, K., and Sorimachi, H. (2006) *J. Biol. Chem.* **281**, 11214-11224
29. Sorimachi, H., Kinbara, K., Kimura, S., Takahashi, M., Ishiura, S., Sasagawa, N., Sorimachi, N., Shimada, H., Tagawa, K., Maruyama, K., and Suzuki, K. (1995) *J. Biol. Chem.* **270**, 31158-31162
30. Masumoto, H., Yoshizawa, T., Sorimachi, H., Nishino, T., Ishiura, S., and Suzuki, K. (1998) *J. Biochem.* **124**, 957-961
31. Sorimachi, H., Toyama-Sorimachi, N., Saido, T. C., Kawasaki, H., Sugita, H., Miyasaka, M., Arahata, K., Ishiura, S., and Suzuki, K. (1993) *J. Biol. Chem.* **268**, 10593-10605
32. Lee, H. J., Sorimachi, H., Jeong, S. Y., Ishiura, S., and Suzuki, K. (1998) *Biol. Chem.* **379**, 175-183
33. Lee, H. J., Tomioka, S., Kinbara, K., Masumoto, H., Jeong, S. Y., Sorimachi, H., Ishiura, S., and Suzuki, K. (1999) *Arch. Biochem. Biophys.* **362**, 22-31
34. Tompa, P., Emori, Y., Sorimachi, H., Suzuki, K., and Friedrich, P. (2001) *Biochem. Biophys. Res.*

Commun. **280**, 1333-1339
35. Schad, E., Farkas, A., Jekely, G., Tompa, P., and Friedrich, P. (2002) *Biochem. J.* **362**, 383-388
36. Friedrich, P., Papp, H., Halasy, K., Farkas, A., Farkas, B., Tompa, P., and Kasa, P. (2004) *Eur. J. Neurosci.* **19**, 1819-1825
37. Ono, Y., Kakinuma, K., Torii, F., Irie, A., Nakagawa, K., Labeit, S., Abe, K., Suzuki, K., and Sorimachi, H. (2004) *J. Biol. Chem.* **279**, 2761-2771
38. Saido, T. C., Nagao, S., Shiramine, M., Tsukaguchi, M., Sorimachi, H., Murofushi, H., Tsuchiya, T., Ito, H., and Suzuki, K. (1992) *J. Biochem.* **111**, 81-86
39. Suzuki, K., Tsuji, S., Kubota, S., Kimura, Y., and Imahori, K. (1981) *J. Biochem.* **90**, 275-258
40. Jones, E. Y., Stuart, D. I., and Walker, N. P. (1989) *Nature* **338**, 225-228
41. Davis, T. L., Walker, J. R., Finerty, P. J., Jr., Mackenzie, F., Newman, E. M., and Dhe-Paganon, S. (2007) *J. Mol. Biol.* **366**, 216-229

FOOTNOTES

*We would like to thank Hiroyuki Kawahara (Hokkaido University), Noriko Toyama-Sorimachi (International Medical Center of Japan), Shoichi Ishiura, Tatsuya Maeda, Keiko Abe (The University of Tokyo), Koichi Suzuki (Toray Inc.), and all of our laboratory members for experimental support and valuable discussion. This work was supported in part by MEXT.KAKENHI 17780115 (to S.H.), 17028055, and 18076007 (to H.S.), by JSPS.KAKENHI 18380085 (to H.S.), by a Sasagawa Scientific Research Grant from The Japan Science Society (to S.H.), by a Research Grant (14B-4) for Nervous and Mental Disorders from the Ministry of Health, Labor and Welfare, and by a Takeda Science Foundation Research Grant (to H.S.).

The abbreviations used are: nCL-2, novel calpain large subunit-2; nCL-4, novel calpain large subunit-4; SDS, sodium dodecyl sulfate; WT, wild type.

FIGURE LEGENDS

Fig. 1. **Purification of recombinant mouse nCL-2.** (A) SDS-PAGE analysis. nCL-2 was expressed in *E. coli* and purified on Ni^{2+}-chelating and MonoQ columns. Samples were separated by SDS-PAGE and stained by CBB. nCL-2 bands are indicated by arrowheads. Lanes: 1, total lysate of nCL-2-expressing *E. coli* BL21/pG-Tf2 cells; 2, its supernatant after centrifugation; 3, an nCL-2 fraction (5 μg) eluted from the Ni^{2+}-chelating column; 4, the final nCL-2 fraction (1.5 μg) after MonoQ column chromatography. An asterisk indicates a host protein still included in the final nCL-2 fraction. (B) Suc-LLVY-MCA hydrolyzing activities of total lysate supernatants (100 μg) of BL21/pG-Tf2 cells transformed with empty pCold vector (mock), or expression vector for inactive nCL-2:C105S (nCL-2CS) or WT nCL-2 (nCL-2). Fluorescence units in vertical axis represent increase in emission at 460 nm ± Ca^{2+} at 20°C for 30 min. (C) "Mock purification" using mock-transformed BL21/pG-Tf2 cell lysate. Samples were separated by SDS-PAGE and stained by CBB. Lanes: S1 and S2, nCL-2- and mock-transformed cell lysate supernatants, respectively; E1–E3, the final Mono Q fractions eluted around 0.2 M NaCl. nCL-2 band is indicated by an arrowhead.

Fig. 2. **Characterization of nCL-2.** In (A), (C), and (E), closed circles, open squares, and triangles represent recombinant nCL-2, μ-calpain, and m-calpain, respectively. (A) Ca^{2+}-dependency of the Suc-LLVY-MCA hydrolyzing activity. The activities were standardized by defining the values at pCa=2 for nCL-2 and m-calpain and pCa=3 for μ-calpain as 100%. (B) Effect of inhibitors on nCL-2 activity. The activities were standardized by defining the activity in the presence of 5 mM EDTA and in the absence of inhibitors as 0% and 100%, respectively. CSTN DI, calpastatin domain I; CSTN pep42, an inhibitory peptide derived from one of four calpastatin-reactive domains. (C) Temperature dependency with a 20-min incubation. Activities were standardized with the values at 20°C defined as 100%. (D) (left) Time course of nCL-2 activity at the indicated temperatures. Activities were standardized with the value at 15°C for 60 min defined as 100%. (right) Amplified view of the left graph in the range from 0 to 2 min of incubation. (E) pH dependency. Activities were standardized with the values at pH=6.0 for nCL-2, pH=7.0 for μ-calpain, and pH=7.3 for m-calpain defined as 100%.

Fig. 3. **Characterization of autolysis of nCL-2.** nCL-2 (0.1 mg/ml) was incubated with or without Ca^{2+} for 0, 10, 30, 60, and 180 sec at 25°C and for 600 sec at 37°C. (A) (left) SDS-PAGE analysis of autolytic fragments stained with CBB. (right) The band intensity of full-length nCL-2 (closed arrowhead) was quantified by densitometry. An asterisk indicates the impurity as also shown in Fig. 1A. (B) Western blot analyses with anti-nCL2 (left), anti-His (middle), and RP2-calpain 8 (right) antibodies. Closed arrowheads and open arrowheads (a-f) indicate full-length and autolytic fragments of nCL-2, respectively. (C) Schematic illustration of the recognition sites for the anti-nCL2, anti-His, and RP2-calpain 8

antibodies, the autolytic sites, and positions of the autolytic fragments obtained above (a-f).

Fig. 4. **nCL-2 forms homo-oligomers.** (A) Elution profile of purified nCL-2 through a gel filtration column. The solid line represents A_{280} of the eluate from the column. Fractions were subjected to SDS-PAGE with CBB staining, and are shown in the upper panel. (B) Schematic illustration of the structures of epitope-tagged wild-type or deletion mutants of nCL-2, mCL, 30K, and 30K-2 used for the immunoprecipitation analyses. (C) HA-mCL (lanes 1 and 2), HA-nCL-2 (lanes 4 and 5), or mock (lane 3) was co-expressed with FLAG-30K (lanes 2, 3, and 5) or mock (lanes 1 and 4) in COS7 cells. The cell lysates were immunoprecipitated (IP) with anti-FLAG agarose and subjected to western blot analysis using anti-FLAG and anti-HA antibodies. (D) FLAG-nCL-2 (lanes 1, 3, and 5) or mock (lanes 2 and 4) was co-expressed with HA-nCL-2 (lanes 2 and 3), myc-nCL-2 (lane 4 and 5), or mock (lane 1) in COS7 cells. The cell lysates were immunoprecipitated (IP) with an anti-FLAG or anti-myc antibody as indicated, and subjected to western blot analysis using anti-FLAG, anti-HA, and anti-myc antibodies. (E) (left) FLAG-nCL-2 (lane 3) or mock (lane 2) was co-expressed with HA-nCL-2 (lanes 2 and 3) in COS7 cells. In this experiment, 0.1 μg of each DNA was used for the transfection. The cell lysates were immunoprecipitated (IP) with anti-FLAG agarose and subjected to western blot analysis using anti-FLAG and anti-HA antibodies. To confirm the expression level of nCL-2 in the transfected cell lysates, 30 μg of each cell lysate was analyzed by western blot using anti-nCL2 antibody (lanes 2 and 3), compared with the same amount of cell lysate prepared from mouse gastric mucosa (lane 1). (right) CBB staining of the cell lysates used. (F) HA-ΔEF5 (lanes 5–7) or HA-nCL-2 (lane 8) was co-expressed with FLAG-ΔEF5 (lanes 6 and 8), FLAG-nCL-2 (lane 7), or mock (lane 5) in COS7 cells. The cell lysates were immunoprecipitated with anti-FLAG agarose and subjected to western blot analysis using anti-FLAG and anti-HA antibodies. Data in lanes 1–3 are essentially the same as lanes 1–3 in (D), but from independent experiments for comparison with lanes 4–8.

Fig. 5. **Domain IV is not required for nCL-2 oligomerization.** Various truncation mutants with a FLAG or HA tag at the N-terminus were co-expressed in COS7 cells in the combinations indicated. Mock was used as a partner for single protein expression. The cell lysates were immunoprecipitated with anti-FLAG agarose and subjected to western blot analysis using anti-FLAG and anti-HA antibodies. (A) The nCL-2 oligomer formed without dIV (lane 3), but was barely detectable when dIII and dIV were deleted (lane 6). (B) Full-length nCL-2 oligomerized with ΔdIV (lane 3), but not with ΔdIII+IV (lane 5), regardless of the types of tag used. (C) dIV of nCL-2 did not form oligomers (lane 3). The expression of dIII of nCL-2 was not as strong as that of other constructs (lanes 6–8, and 10), but the faint dIII co-precipitated with dIII (lane 8) or full-length nCL-2 (lane 10).

Fig. 6. **Effect of oligomerization on nCL-2 activity.** (A) HA-nCL-2 was co-expressed with

FLAG-nCL-2 in COS7 cells, and the cell lysates were immunoprecipitated with anti-FLAG agarose. The precipitant was then incubated for 0 (lane 1), 30 (2), 60 (3), and 120 min (4 and 5) with or without Ca^{2+} as indicated, and subjected to western blot analysis using anti-FLAG and anti-HA antibodies. Closed and open arrowheads indicate full-length and autolyzed nCL-2, respectively. (B) HA-nCL-2CS (lanes 2, 3, 5, and 6) or mock (lanes 1 and 4) was co-expressed with FLAG-nCL-2CS (lanes 3 and 6) or mock (lanes 2 and 5) in COS7 cells. The cell lysates were immunoprecipitated with anti-FLAG agarose, and the protein-bound anti-FLAG agarose was incubated with (lanes 4–6) or without (lanes 1–3) Ca^{2+}, then washed with the same buffer. The protein remaining on the agarose was subjected to western blot analysis using anti-FLAG and anti-HA antibodies.

Fig. 7. **nCL-2 does not bind 30K-2.** HA-nCL-2 (lanes 2 and 3), HA-mCL (lanes 5 and 6), or mock (lanes 1 and 4) was co-expressed with FLAG-30K-2 (lanes 1, 3, 4, and 6) or mock (lanes 2 and 5) in COS7 cells. The cell lysates were immunoprecipitated with anti-FLAG agarose and subjected to western blot analysis using anti-FLAG and anti-HA antibodies.

Table 1. Summary of interactions between nCL-2 and its mutants

		(FLAG-tagged)						
		FL	FL-C105S	ΔEF5	ΔdIV	ΔdIII+IV	dIV	dIII
(HA-tagged)	FL	++	n	++	++	-	-	+
	FL-C105S	n	++*		n	n	n	n
	ΔEF5	++	n	++	n	n	n	n
	ΔdIV	++	n	n	++	n	n	n
	ΔdIII+IV	-	n	n	n	-	n	n
	dIV	-	n	n	n	n	-	n
	dIII	+	n	n	n	n	n	+

FL: full-length; n: not tested

++, +, and -: abundantly, weakly, and not detected, respectively, in the absence of Ca^{2+}

*: both in the presence and absence of Ca^{2+}

Hata *et al.* Fig. 1

(A)

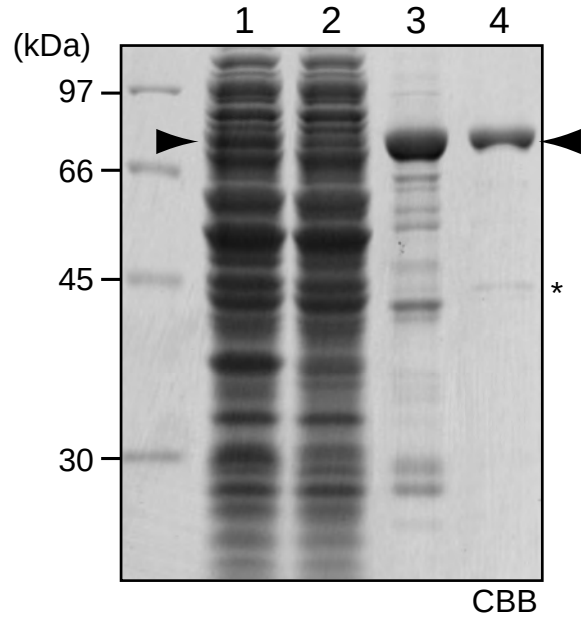

(B)

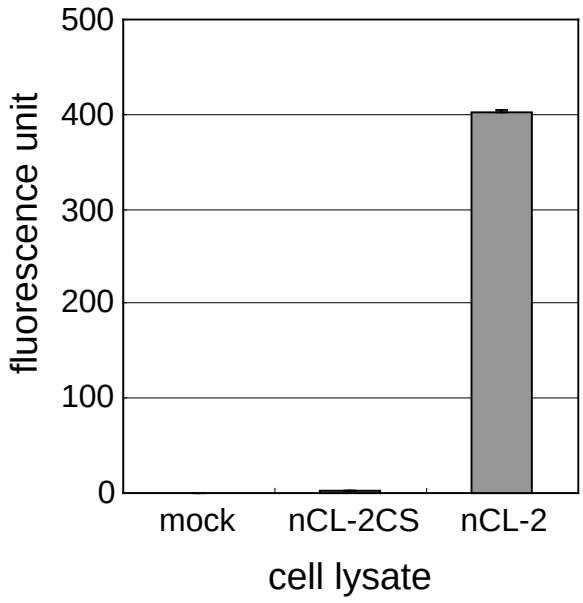

(C)

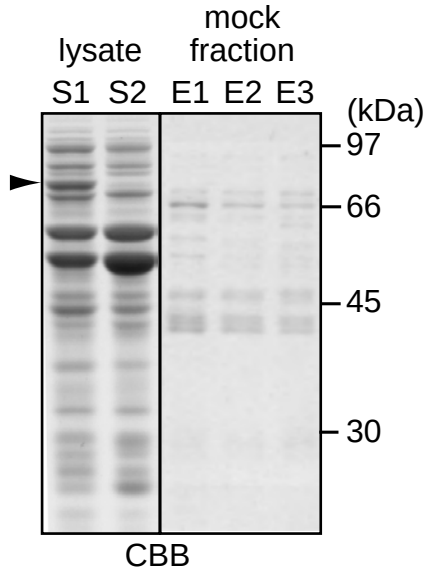

Hata *et al.* fig.2

(A)

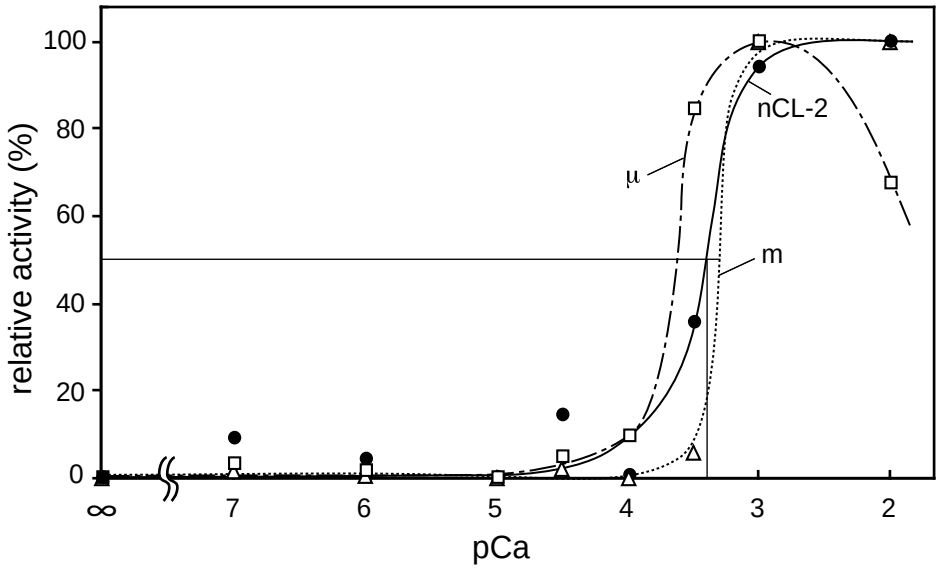

(B)

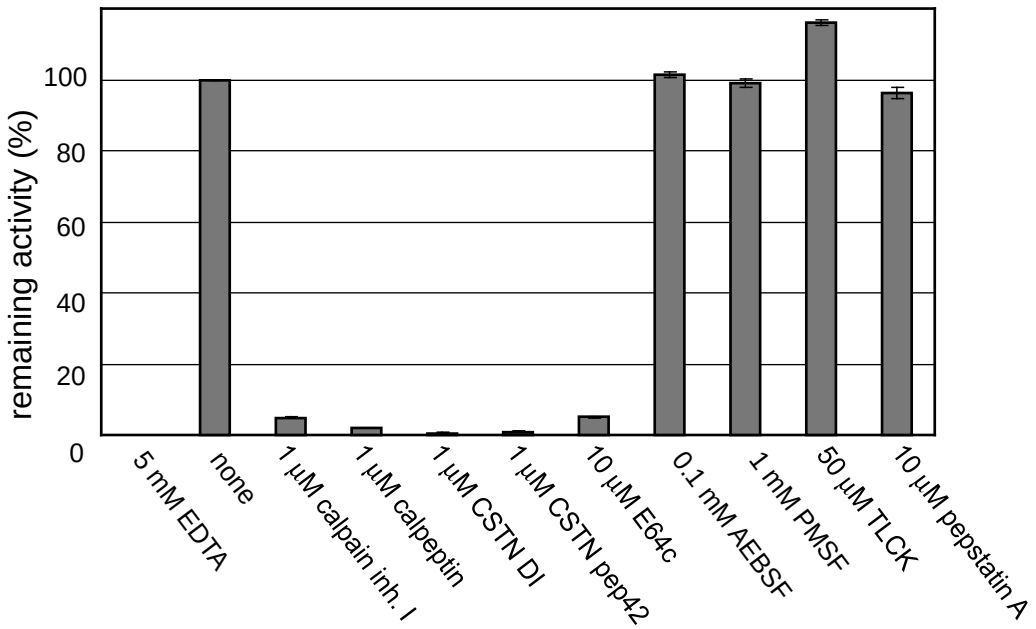

Hata *et al.* fig.2 (continued)

(C)

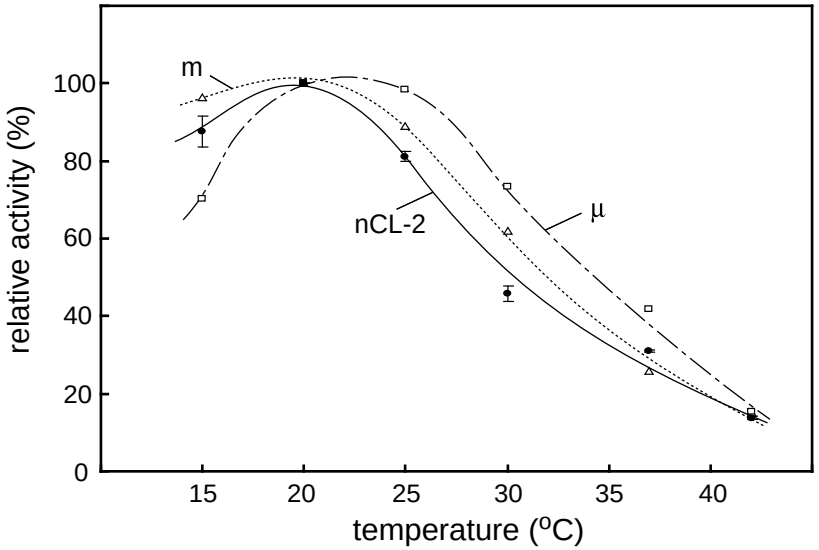

(D)

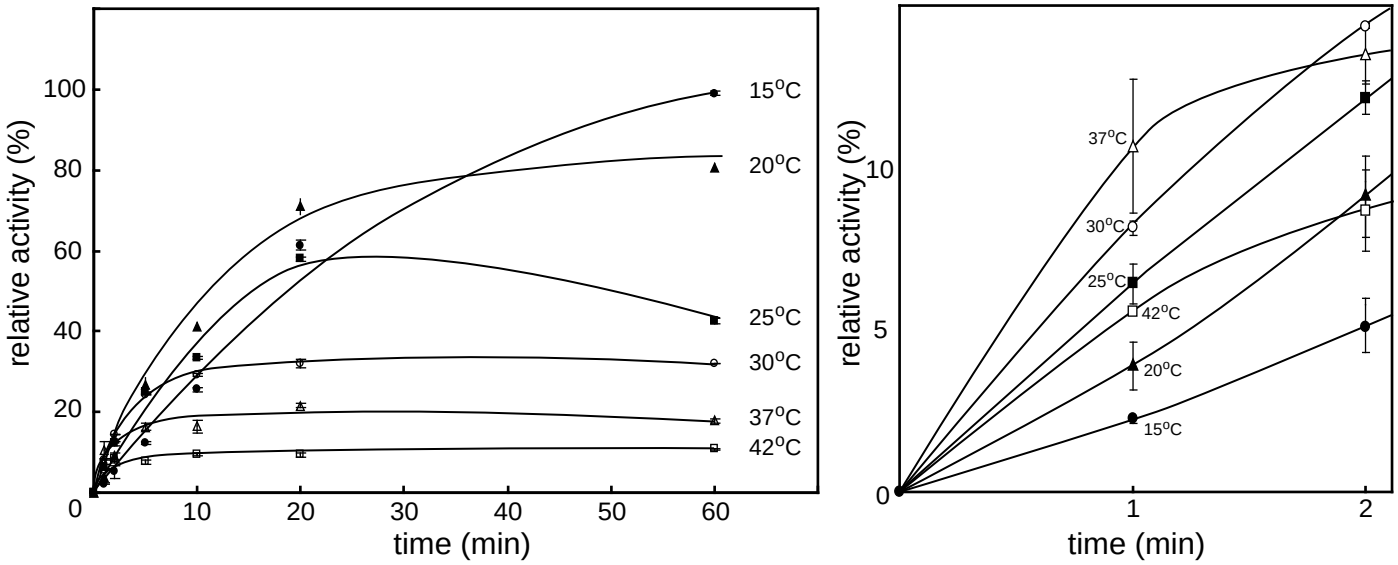

(E)

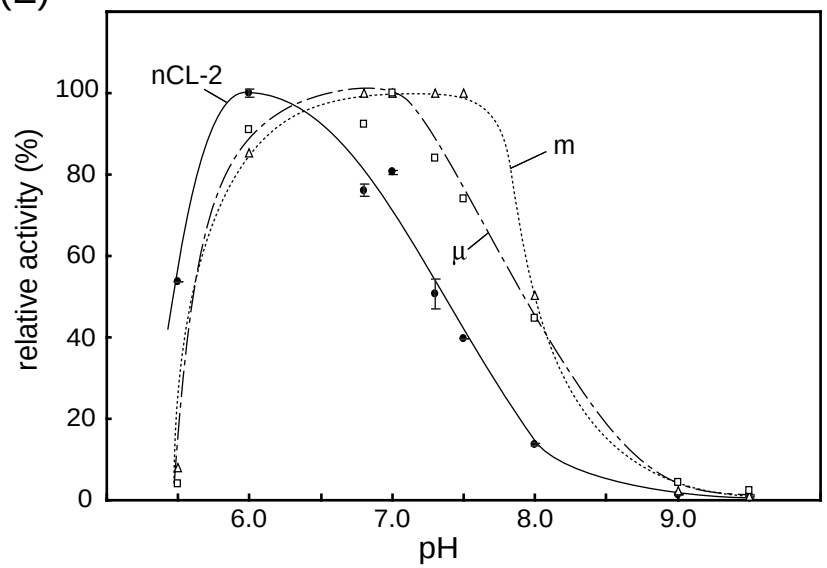

Hata *et al.* fig. 3

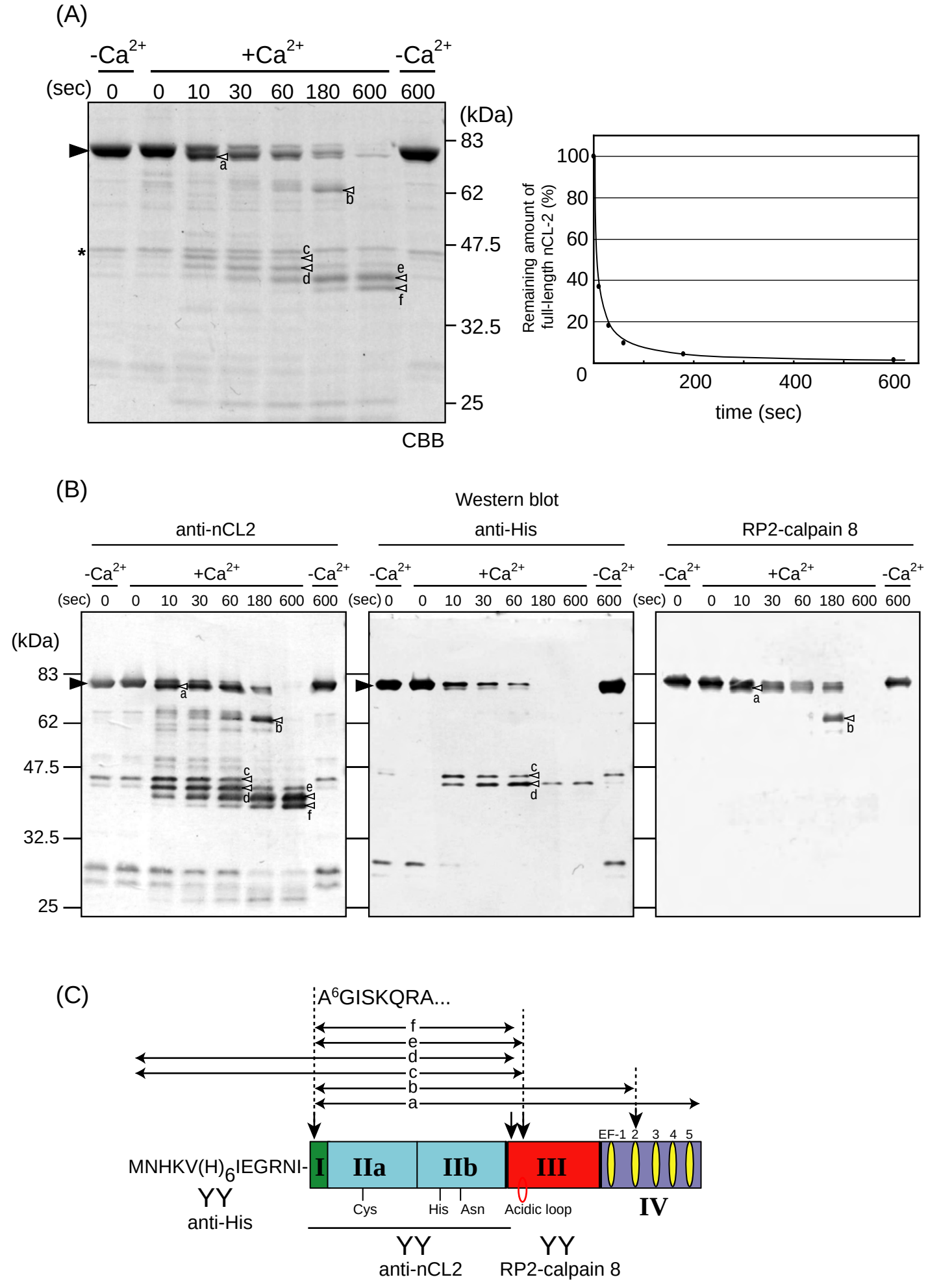

Hata *et al.* fig. 4

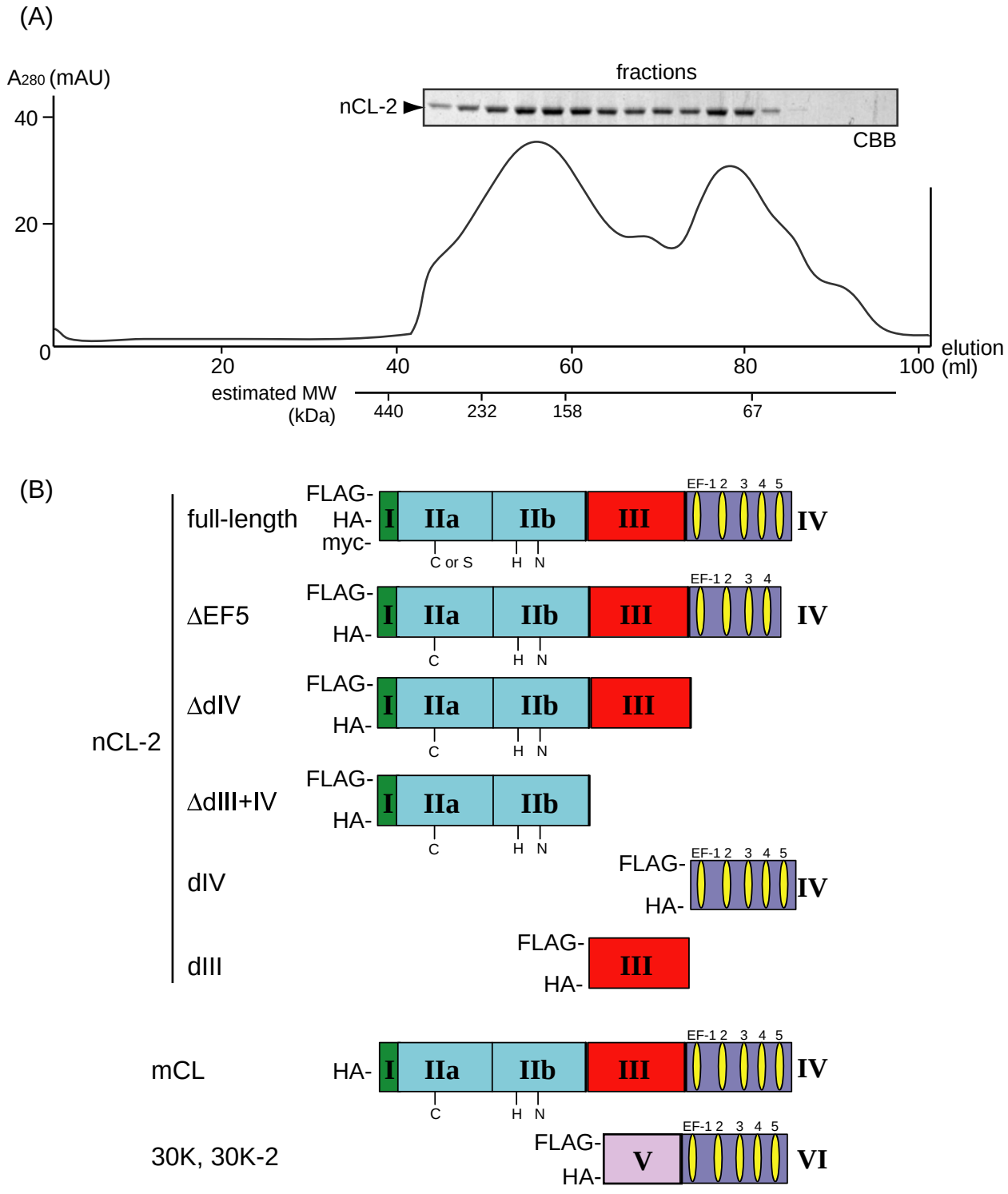

Hata *et al.* fig. 4 (continued)

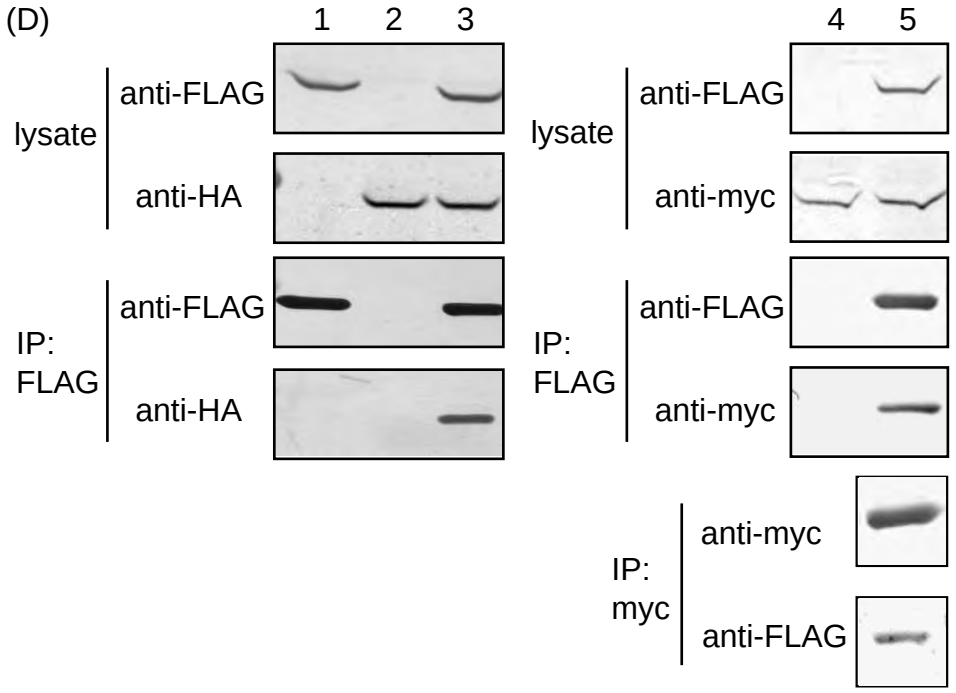

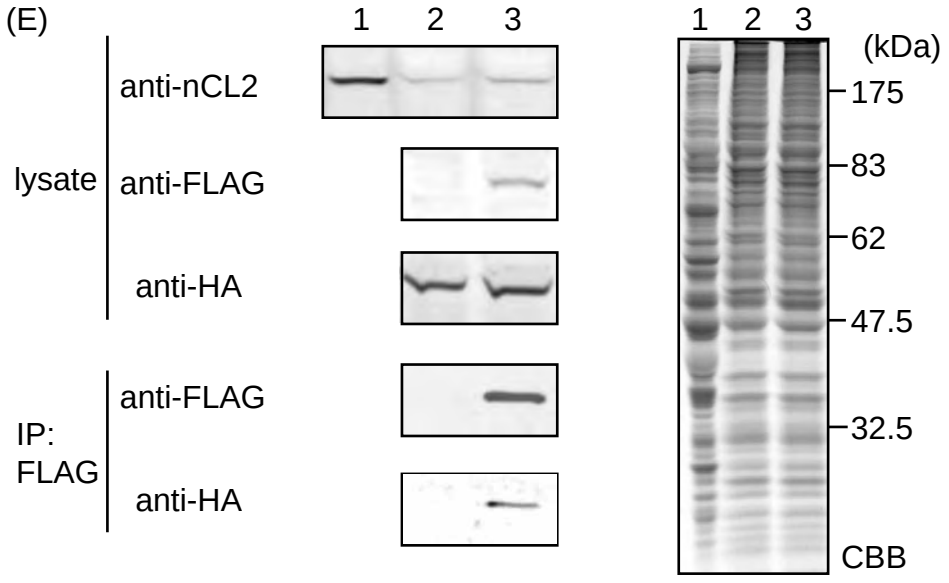

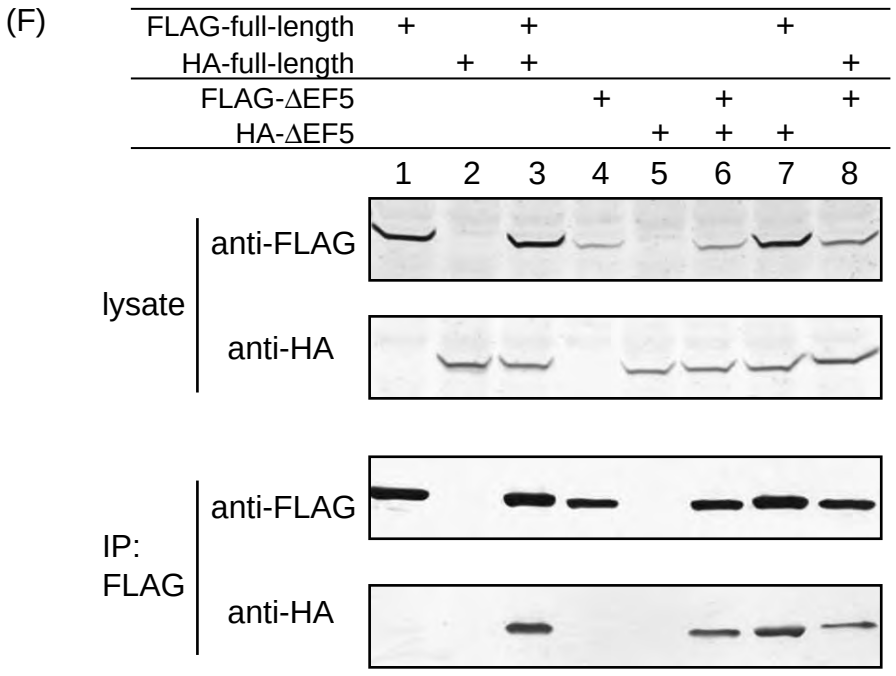

Hata *et al.* fig. 5

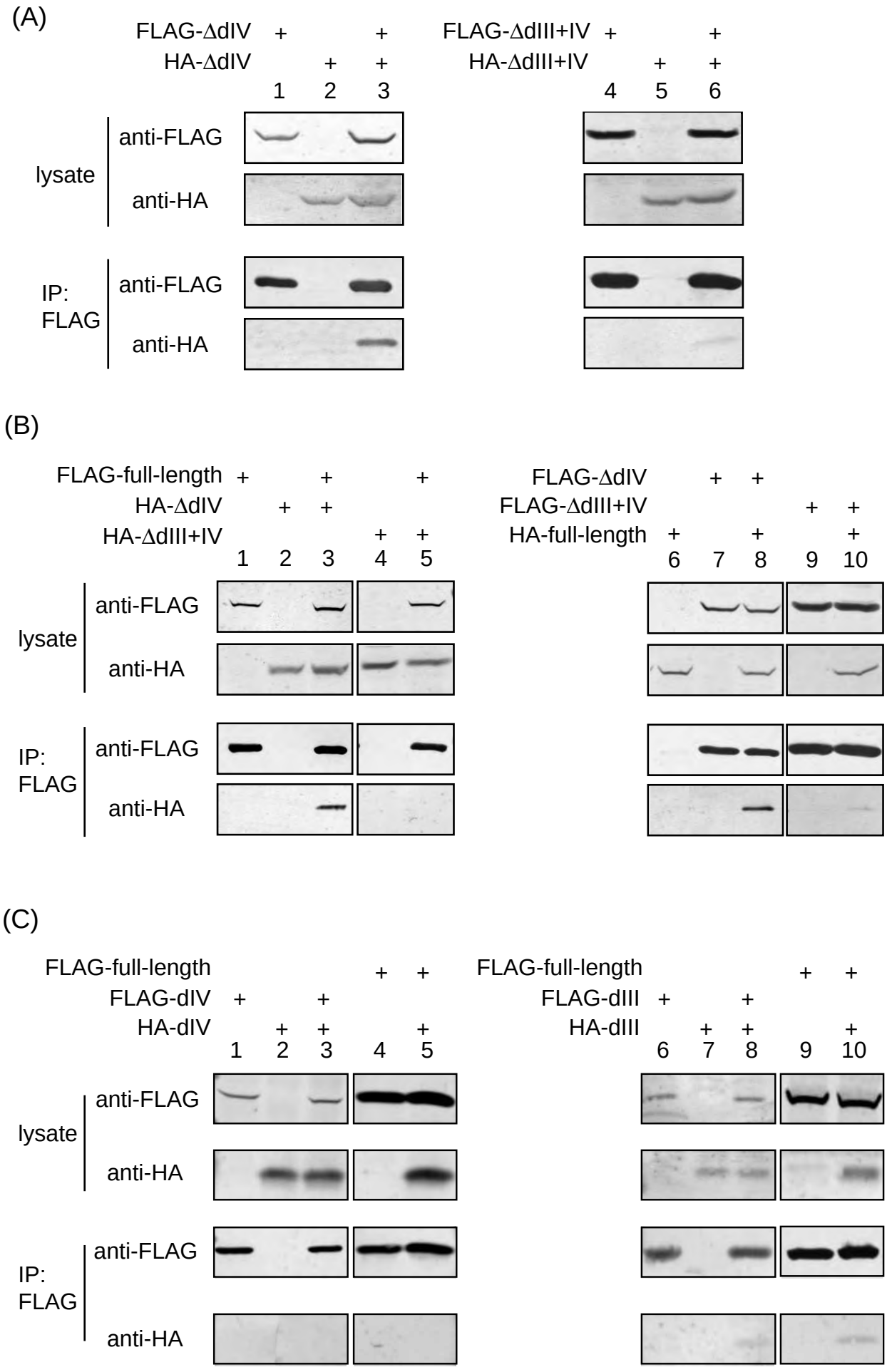

Hata *et al.* fig. 6

(A)

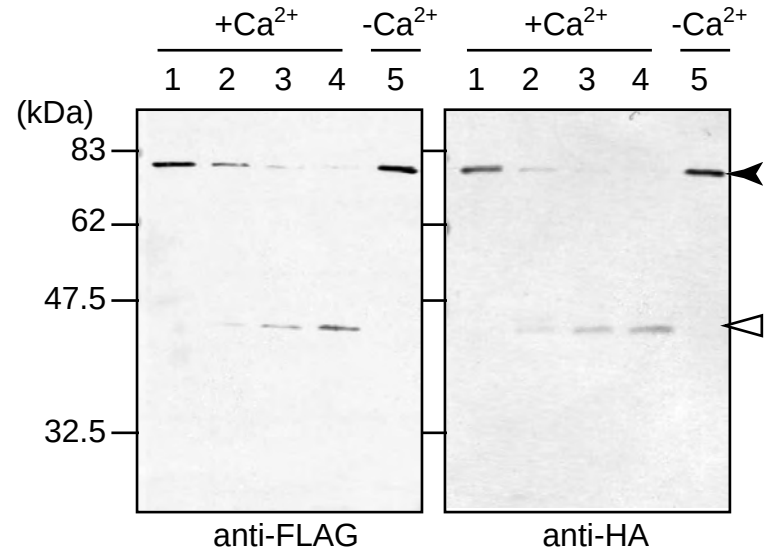

(B)

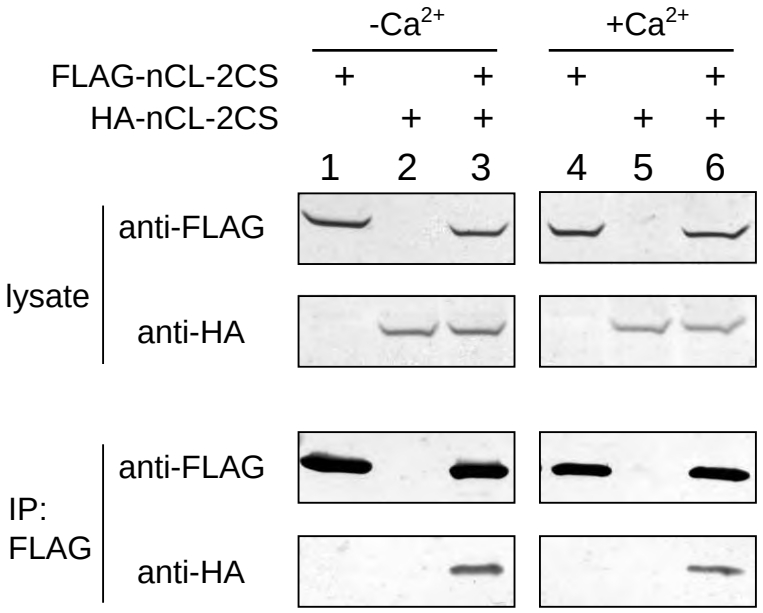

Hata *et al.* fig.7